Semiconductor Physics, Quantum Electronics & Optoelectronics, 2010. V. 13, N 4. P. 337-342.

PACS 73.40.Cg, 73.40.Ns, 85.30.-z

Formation of ohmic contacts to *n*(*p*)-gan and measurement of their contact resistivity

M.S. Boltovets[1], V.M. Ivanov[1], R.V. Konakova[2], Ya.Ya. Kudryk[2], V.V. Milenin[2], V.V. Shynkarenko[2], V.M. Sheremet[2], Yu.N. Sveshnikov[3], B.S. Yavich[4]
[1]*State Enterprise Research Institute "Orion", 8a Eugene Pottier St., Kyiv 03057, Ukraine,*
[2]*V. Lashkaryov Institute of Semiconductor Physics, NAS Ukraine*
41 Prospect Nauky, Kyiv 03028, Ukraine
Tel.: (380-44) 525-61-82; Fax: (380-44) 525-83-42; e-mail: konakova@isp.kiev.ua,
[3]*Close Corporation "Elma-Malakhit", Zelenograd, Russia; e-mail: info@emal.zelcom.ru*
[4]*Close Corporation "Svetlana-Optoelektronika", Sankt-Peterburg, Russia*

Abstract. We propose multilayer ohmic contacts to *n*- and *p*-GaN layers, with titanium boride as diffusion barrier. It is shown that the optimal method of contact resistivity measurement is the transmission line method (TLM) with circular contact geometry. The Ti–Al–TiB_x–Au contact metallization to *n*-GaN retains its layer structure after thermal annealing at temperatures up to 900 °C. The contact resistivity ρ_c is $(6.69\pm1.67)\times10^{-5}$ $\Omega\cdot cm^2$. For the Au–TiB_x–Ni–*p*-GaN contact structure, the contact resistivity is $(1\pm0.15)\times10^{-3}$ $\Omega\cdot cm^2$.

Keywords: ohmic contact, gallium nitride, contact resistivity, transmission line method.

Manuscript received 22.07.10; accepted for publication 02.12.10; published online 30.12.10.

1. Introduction

In recent years, the lighting engineering dealing with production of light-emitting diodes (LEDs) for various purposes has been developing intensely. Having higher light efficiency and longer service life, LEDs rather actively displace other illuminators such as incandescent and luminescent lamps [1, 2]. The process has become more evident after appearance of highly efficient LEDs based on the III group nitrides that made it possible to develop blue LEDs and, closing the RGB range, obtain white light using concurrently red, green and blue LEDs. Such three-color cells are of importance for developing of LED monitors.

It is known that one cannot realize such properties of gallium nitride (that is the most advanced material of the III group nitrides) as high value of avalanche breakdown field and thermal stability without highly reliable ohmic contacts. The reason is that application of LEDs for illumination requires increase of power of the present-day diodes. In this case, LED heating in both the base region and contacts will lead to device degradation. Therefore, search for contact metallization systems to gallium nitride LEDS that would be high-tech, thermally stable and compatible with technological processes for microwave devices makes a topical problem.

Another (no less important) problem in development of investigations of contact metallization to GaN is making of low-resistance thermally stable contacts to *p*-GaN. The existing experimental data on the resistivity ρ_c for contacts to *p*-GaN indicate wide spread of ρ_c values depending on the level of doping with acceptor impurity and crystallographic orientation of GaN surface as well as on the work function φ_m of the material of contact-forming layer. The latter can be formed with multicomponent compounds with high φ_m value [3-8].

Reduction of resistivity ρ_c of contact to *p*-GaN can be achieved (along with choosing the appropriate value of φ_m) by doping the near-surface layer with an acceptor impurity that provides tunnel current transport in the ohmic contact. The theoretical studies of ρ_c for contact to *p*-GaN showed [8] that, in the case of a tunnel contact and with allowance made for tunneling of light and heavy holes, ρ_c value depends on the crystallographic orientation of GaN. The calculated ρ_c value of about 2×10^{-4} $\Omega\cdot cm^2$ corresponds to concentration of noncompensated acceptors ~10^{19} cm^{-3} for GaN [0001] and 5×10^{18} cm^{-3} for GaN [1010], respectively.

© 2010, V. Lashkaryov Institute of Semiconductor Physics, National Academy of Sciences of Ukraine

At the same time, it turned out that, along with the well-known mechanisms of current transport in ohmic contacts to *n*-GaN grown on sapphire, metallic conductance is observed in such contacts over a wide temperature range. The reason is high density of structural defects in GaN. Increase of ρ_c as temperature grows (and contributes to device structure heating) is undesirable not only for LEDs but for other types of GaN-based electronic devices as well. Thus, formation of metal–GaN interface with preset parameters as well as making of buffer layers (diffusion barriers) between the upper metallization layer and contact-forming layer that impede mass transfer of contact components are topical from the viewpoint of production of highly reliable thermally stable ohmic contacts to *n*(*p*)-GaN epitaxial layers grown on foreign substrates.

Therefore, one should use multilayer contact metallizations (made of refractory metals and their compounds) serving as diffusion barriers. In this connection, borides and nitrides of refractory metals seem most promising [9-11]. Choice of procedures and estimation of ρ_c measurement errors are of great importance too. In this work, we studied efficiency of TiB_x as diffusion barrier in ohmic contacts to GaN using the transmission line method (TLM) to measure ρ_c.

2. Methods of contact resistance measurement

Contact resistivity is one of the main parameters that characterizes both an ohmic contact and processes of heat release in it. The principal difficulty in measurement of contact resistance is its determination from the measured resistance *R*. The latter can be represented as a sum of resistances of the contacts (R_c), semiconductor (R_s), probes and lead-ins (R_p) and the resistance provoked by current spreading (R_T) [12]:

$$R = R_c + R_s + R_T + R_p \,. \quad (1)$$

It was shown in [13] that the biggest error in determination of contact resistivity is characteristic of the method with vertical geometry of test structure (the Cox–Strack method) [14-16]. In this method, the minimal relative error of ρ_c measurement (at $\rho_c/\rho_s = 0.01$ cm, where ρ_s is the semiconductor resistivity) is as high as 90% if one uses lithography with accuracy of 2.5 μm [13]. Therefore, it is reasonable to apply the Cox–Strack method [14] only if one has to measure the parameters of contacts to bulk material and in the case $\rho_c \geq \rho_s$. The minimal value of error is ensured by the method of interface probing [17] and Kelvin method [16, 18, 19]. At $\rho_c/\rho_s = 0.01$ cm, the relative error of ρ_c measurement is 25% and 15%, respectively, if one uses lithography with accuracy of 2.5 μm [13]. When using the probing method, the lithography should enable one to deposit sufficiently small external terminals, while application of the Kelvin method for measurement of low resistances requires contacts smaller than 1 μm×1 μm [19].

The most convenient and sufficiently accurate methods are those TLM versions [20-27] that make it possible to measure low contact resistances, and the lithography used meets the requirements to making test structures for measurements. TLM has many modifications that differ in geometry and ρ_c calculation technique. One should set off the versions of TLM with linear and circular contact geometry.

The necessary condition for resistance measurement by TLM with linear geometry of contact pads is absence of edge surface spreading of current. To this end, each group of contacts has to be separated from the rest part of semiconductor plate. This requires application of additional technological process. Contrary to this, use of structures with circular geometry of contact pads makes it possible to avoid edge spreading of current without additional treatment [25, 26].

In the TLM with circular geometry, the resistance between contact pads is determined with the following expression [25]:

$$R = \frac{R_{SH}}{2\pi}\ln\frac{r_2}{r_1} + \frac{R_{SH}}{2\pi}\frac{1}{\alpha r_1}\frac{I_0(\alpha r_1)}{I_1(\alpha r_1)} \quad (2)$$

Here r_1 (r_2) is the inner (outer) radius of the corresponding contact pad, $I_0(\alpha r_1)$ and $I_1(\alpha r_1)$ the modified Bessel functions of the zeroth and first order, respectively, $\alpha = 1/L_T$ the damping coefficient, $L_T = \sqrt{\rho_c t/\rho_s}$ transfer length, *t* thickness of the semiconductor epitaxial layer.

If $L_T >> r_1$ and $\ln(r_2/r_1) = C$, then the approximation $I_0(\alpha r_1)/I_1(\alpha r_1) \to 2/\alpha r_1$ is valid, and the resistance measured is determined as [25]:

$$R = \frac{CR_{SH}}{2\pi} + \frac{\rho_c}{\pi r_1^2}\,. \quad (3)$$

Thus, by plotting the dependence $R = f\left(1/\pi r_1^2\right)$, one can calculate ρ_c from the slope of the straight line. If $L_T \leq r_1$, then the value obtained in the above way will give the upper estimate for contact resistivity [25].

One should note that, to determine contact resistivity accurately, the difference between the outer and inner radii of contact pad has to be minimal. In that case, the contribution from semiconductor resistance to the total resistance becomes smaller [21]. The relative error of contact resistivity measurement can be determined from the following expression [13]:

$$\frac{\Delta\rho_c}{\rho_c} = 2\frac{\Delta l}{r} + \frac{\Delta R}{R} + \frac{\rho_s}{\rho_c}\frac{Cr^2}{2t}\left(\frac{\Delta R}{R} + \frac{\Delta t}{t}\right), \quad (4)$$

where Δt is inaccuracy of the grown epitaxial layer thickness, Δl inaccuracy of lithography when depositing contacts. The results of calculation of the dependence $f(r) = \Delta\rho_c/\rho_c$ are shown in Fig. 1. At best, if $\rho_c/\rho_s = 0.01$ cm^{-1}, the relative inaccuracy of ρ_c measurement is 28%.

© 2010, V. Lashkaryov Institute of Semiconductor Physics, National Academy of Sciences of Ukraine

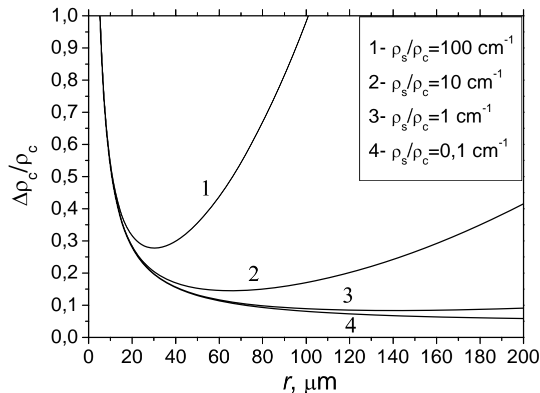

Fig. 1. Dependence of relative inaccuracy of contact resistivity measurement on contact radius when using TLM with circular contact geometry [13].

If one uses TLM with linear geometry of contact pads and ρ_c/ρ_s = 0.01 cm and $\rho_s = 10^{-4}$ Ω·cm, the relative inaccuracy of ρ_c measurement is 16% [13]. This value is below that obtained in the case of TLM with circular geometry. However, as ρ_s increases to 10^{-2} Ω·cm, the relative inaccuracy in the case of TLM with linear geometry grows to 50%, contrary to the case of TLM with circular geometry in which the error does not depend on the value of semiconductor resistivity.

3. Formation of contact systems

To measure resistivity of ohmic contacts to *n*- and *p*-GaN, we chose TLM with circular geometry of contact pads. We made a test pattern with circular geometry of contacts (Fig. 2) and test TLM structures to measure ρ_c.

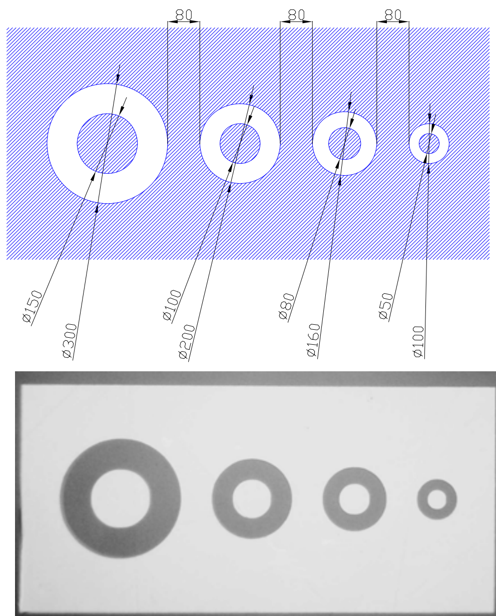

Fig. 2. Contact structure pattern for ρ_c measurement (a) and design of a contact structure formed on GaN to measure ρ_c (b). (The sizes are given in μm.)

The GaN epitaxial structures were MOCVD-grown on the sapphire (0001) substrates 400 μm thick. The LED structures were made at the Close Corporation "Svetlana-Optoelektronika", Sankt-Peterburg, Russia. A low-temperature nucleating layer, *n*-GaN layer (3.5 μm), active area with five InGaN/GaN quantum wells, *p*-AlGaN current-limiting layer (20 nm) and *p*-GaN layer (0.1 μm) with dopant concentration > 2×10^{17} cm^{-3} were grown successively on the sapphire substrate. The n^+-*n*-n^+-GaN–Al_2O_3 epitaxial structures were grown at the Close Corporation "Elma-Malakhit", Zelenograd, Russia. The layer parameters were as follows: $n^+ \approx 10^{18}$ cm^{-3}, $d_{n+} \approx 0.8$ μm; $n \approx 10^{17}$ cm^{-3}, $d_n \approx 3$ μm; buffer layer: $n^+ \approx 10^{18}$ cm^{-3}, $d_{n+} \approx 3$ μm.

The dislocation density in structures of both types was over 10^8 cm^{-2}. The successive Ti–Al–TiB_x–Au (Ni–TiB_x–Au) metallization layers to form ohmic contact to n^+-GaN (*p*-GaN) were deposited with magnetron sputtering in the argon atmosphere onto the gallium nitride surface subjected to photon cleaning. After sputtering the Ti–Al (Ni) layer to *n*-GaN (*p*-GaN), the samples were subjected to rapid thermal annealing (RTA) at T = 900 °C in the nitrogen atmosphere for 30 s. Then the TiB_x and Au layers were deposited. As a result, the ohmic contacts Au–TiB_x–Al–Ti-*n*-GaN and Au–TiB_x–Ni–*p*-GaN were formed.

The contact resistivity was studied for the Au–TiB_x–Al–Ti–*n*-GaN contact structures before and after RTA at T = 700°C, 870°C and 900°C for 60 s and Au–TiB_x–Ni–*p*-GaN contact structures before and after RTA at 700°C for 60 s. We used the developed plant for measurement of parameters of ohmic contacts to semiconductors (Fig. 3), as well as Auger electron spectroscopy with ion etching by an argon beam (energy of 1 keV) to determine concentration depth profiles of metallization components.

Fig. 3. The plant for measurement of parameters of ohmic contact to semiconductor.

© 2010, V. Lashkaryov Institute of Semiconductor Physics, National Academy of Sciences of Ukraine

4. Structure of contacts before and after RTA

It was shown in [29] that the contacts with TiB_x antidiffusion layer (barrier) demonstrate better thermal stability than those with more widespread metallization with Ti and Al as diffusion barrier. As in [29], our analysis of the concentration depth profiles for components of the Ti–Al–TiB_x–Au contacts to *n*-GaN taken before and after RTA at T = 700 °C in the nitrogen atmosphere for 60 s showed that no interactions between phases in the contact metallization. Some changes in the layer structure of such contact were observed after RTA at a temperature of 900 °C only. One should also note considerable oxygen concentration in the TiB_x layer. Therefore, one may assume presence of titanium oxyboride instead of single-phase of TiB_2 in it. This may be the reason for contact metallization structural failure in the course of RTA at a temperature of 900 °C.

It was noted in a number of works [3-5, 30-32] that formation of ohmic contact to *n*-GaN with contact-forming layers of Al–Ti occurs owing to appearance at RTA of TiN composition whose work function is 3.87 eV, i.e., below that of pure Ti (3.95 eV). In this case, nitrogen vacancies are produced in the GaN near-surface layer because of N atoms coming to the titanium film. These nitrogen vacancies are shallow donors in *n*-GaN. They produce a thin n^+-layer in the near-contact region, thus ensuring, along with TiN, barrier lowering and decrease of ρ_c. In our case, however, the x-ray diffraction pattern had no indications at presence of TiN phase. This may be owing to either small amount of titanium nitride or quasi-amorphous nature of the compound obtained.

Formation of ohmic contact to *p*-GaN at RTA of nickel film occurs due to production of intermetallic compounds of nickel and gallium, with appearance in the GaN near-contact region of gallium vacancies serving as acceptors [6, 7].

5. Electrophysical properties of ohmic contacts

5.1. Au–TiB_x–Al–Ti–n^+-n-n^+-GaN ohmic contacts.

The *I–V* curves of Ti–Al–TiB_x–Au contacts to the n^+-n-n^+-GaN structure taken in the 90–380 K temperature range turned out to be linear over the whole this range. The contact resistivity at room temperature was $(6.69\pm1.67)\cdot10^{-5}$ $\Omega\cdot cm^2$ (Fig. 4). The semiconductor resistivity estimated from the dependence $R(1/\pi r^2)$ was $\sim10^{-2}$ $\Omega\cdot$cm.

The current through the Au–TiB_x–Al–Ti–n^+-n-n^+-GaN contact structure is determined by the semiconductor resistance because structure conductance increases as temperature grows up to 150 K. Further temperature increase led to decrease of conductance. This fact correlates with the temperature dependence of electron mobility in GaN considered in [33].

The contact resistivity measurements in the 225–380 K temperature range showed that there are two regions of ρ_c variation. In the 225–335 K temperature

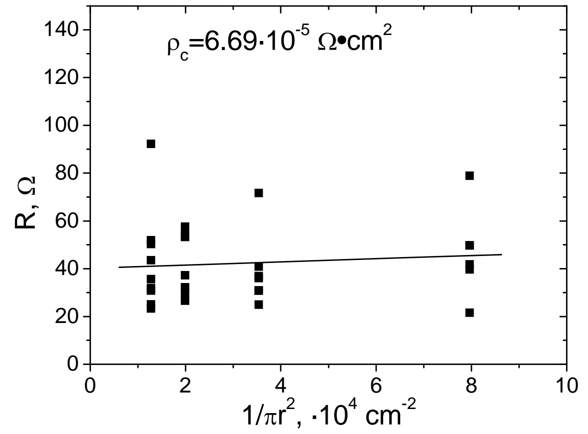

Fig. 4. The total resistance of Au–TiB_x–Al–Ti–*n*-GaN contacts as function of $\dfrac{1}{\pi r^2}$.

range, ρ_c practically does not depend on temperature. This is characteristic of the tunnel mechanism of current transport in the contact. In the 335–380 K temperature range, ρ_c decreases exponentially with temperature and is linear in the coordinates $\ln(\rho_c T) = f(1/T)$. This is characteristic of the thermionic mechanism of current transport. The potential barrier height φ_B determined from the dependence $\ln(\rho_c T) = f(q/kT)$ in the 335–380 K temperature range was 0.16 eV.

In the 225–335 K temperature range, the tunnel mechanism via dislocations of current transport is characteristic of the contact structure. The dislocation density in some samples was $\sim10^8$ cm^{-2}. The current transport mechanism via dislocations was observed in [34] for gallium nitride Schottky barrier diodes. In that case, the dislocation density in GaN was $\sim10^8$–10^{10} cm^{-2}. Such mechanism was advanced earlier to describe the temperature dependence of saturation current in the GaP-based surface-barrier diodes [35].

For the best gallium nitride epitaxial structures with Au–TiB_x–Al–Ti–*n*-GaN ohmic contacts, the contact resistivity was $\sim10^{-6}$ $\Omega\cdot cm^2$. After repeated RTA of the Au–TiB_x–Al–Ti–*n*-GaN contacts at T = 700 °C and T = 870 °C, the current transport mechanism and ohmic contact parameters did not change considerably. This indicates their thermal resistance.

5.2. Au–TiB_x–Ni–p-GaN ohmic contacts.

The *I–V* curves of the Au–TiB_x–Ni–*p*-GaN contact structure subjected to RTA at T = 700 °C for 60 s were linear. The contact resistivity was $(1\pm0.15)\times10^{-3}$ $\Omega\cdot cm^2$ (Fig. 5). This is much higher than that of the ohmic contacts to *n*-GaN; the ρ_s value estimated from the cutoff in the $R(1/\pi r^2)$ curve is $\sim10^{-2}$ $\Omega\cdot$cm. This value is in agreement with the data of other authors who studied ohmic contacts formed in the course of thermal annealing (at T = 700 °C) of a gilded nickel film (Au–Ni) deposited onto the surface of *p*-GaN with $p\approx$

© 2010, V. Lashkaryov Institute of Semiconductor Physics, National Academy of Sciences of Ukraine

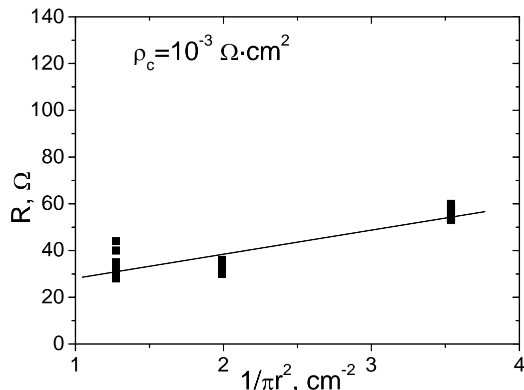

Fig. 5. The total resistance of Au–TiB$_x$–Ni–*p*-GaN contacts as function of $\frac{1}{\pi r^2}$.

10^{17} cm^{-3} [36]. In that case, the contact was formed by the Ga_4Ni_3, Ga_3Ni_2, GaAu and $GaAu_2$ intermetallic phases that reduce the barrier at the interface between the above phases and *p*-GaN. Production of Ga vacancies in the near-contact region that serve as acceptors [7] also favors reduction of ρ_c to *p*-GaN.

When comparing our data on ρ_c value with those of other authors [6, 7], one may assume that in our case, with TiB$_x$ diffusion barrier, the contact-forming layer (after RTA at T = 700 °C) is formed by the $GaNi_3$ and Ga_3Ni_2 intermetallic phases, since the TiB$_x$ layer prevents from penetration of Au atoms to the interface between Ni and GaP. However, this should be confirmed with x-ray diffraction studies. In this case, one should not exclude also additional (positive) influence of Ga vacancies in the *p*-GaN near-contact region on decrease of ρ_c. The repeated RTA (700 °C, 60 s) did not change ρ_c value for the Au–TiB$_x$–Ni–*p*-GaN ohmic contact. This fact indicates completeness of metallurgical reactions in the near-contact region and at the metal–GaN interface in the course of the first RTA.

The fact that ρ_c values are higher than those in the ohmic contact to *n*-GaN is determined by the features of doping of *p*-GaN, e.g., owing to impurities passivation by hydrogen atoms in the course of MOCVD-growth and doping of GaN with uncontrolled donor impurities [37]. The complication results also from absence of metals with work function over 7.5 eV. Therefore, to make low-barrier ohmic contacts to *p*-GaN, one should either use contact-forming compounds with high work function values or form a heavily doped narrow-gap near-surface layer in GaN [3-5, 30].

6. Conclusion

A comparison between the methods of measurement of contact resistivity of ohmic contacts to *n*(*p*)-GaN showed that TLM with circular contact geometry is optimal. Using the developed plant for measurement of ohmic contact parameters, we applied this method for study of electrophysical properties of ohmic contacts to *n*- and *p*-GaN. The contacts were multilayer Au–TiB$_x$–Al–Ti–*n*-GaN structures (that remained thermally stable after RTA at temperatures up to 900 °C [29]) and Au–TiB$_x$–Ni–*p*-GaN structures (that remained thermally stable after RTA at temperatures up to 700 °C). The *I–V* curves of the Ti–Al–TiB$_x$–Au contacts to the n^+-n-n^+-GaN structure were linear in the 90–380 K temperature range; the contact resistivity ρ_c at room temperature was $(6.69\pm1.67)\times10^{-5}$ Ω·cm^2. For the Au–TiB$_x$–Ni–*p*-GaN contact structure, ρ_c = $(1\pm0.15)\times10^{-3}$ Ω·cm^2, and the contact *I–V* curves were.

Thus, the experimental results obtained by us indicate high thermal stability of ohmic contacts, with titanium boride as diffusion barrier, to *n*- and *p*-GaN layers.

Acknowledgements

This work was supported by the Project No 31/4.2.3.1/33 of the Governmental task scientific and technical program “Development and implementation of energy-saving light sources and illumination systems based on them” (Regulation of the Cabinet of Ministers of Ukraine No 632 from July 9, 2008). The development of varactor diodes was carried out under the INCO–COPERNICUS Program (Project No 977131 “MEMSWAVE”).

References

1. F.E. Shubert, *Light-Emitting Diodes*, Cambridge University Press (2006).
2. Yu. Davidenko, High-efficiency modern LEDs // *Sovremennaya Elektronika* no 8, p. 36-43 (2004) (in Russian).
3. H. Morkoç, *Handbook of Nitride Semiconductors and Devices*, Willey-VCH (2008).
4. V.N. Danilin, Yu.P. Dokuchaev, T.A. Zhukova, M.A. Komarov, *High-Power High-Temperature Capable and Radiation-Resistant Microwave New-Generation Devices with AlGaN/GaN Wide-Gap Heterojunction Structures. Reviews of Electronic Equipment*, GUP NPP “Pulsar”, Moscow (2001) (in Russian).
5. Yu.G. Shretter, Yu.T. Rebane, V.A. Zykov, V.G. Sidorov, *Wide-Gap Semiconductors*, Nauka, Sankt-Peterburg (2001) (in Russian).
6. T.V. Blank, Yu.A. Gol’dberg, Semiconductor photoconverters for ultraviolet spectral region. A review // *Fiz. Tekh. Poluprov.* **37**(9), p. 1025-1055 (2003) (in Russian).
7. T.V. Blank, Yu.A. Gol’dberg, The mechanism of current transport in ohmic metal–semiconductor contacts. A review // *Fiz. Tekh. Poluprov.* **41**(11), p. 1281-1308 (2007) (in Russian).
8. N. Mochida, T. Honda, T. Shirasawa, A. Inoue, T. Sakaguchi, F. Koyama, K. Iga // *J. Cryst. Growth* **189-190,** p. 716(1998).

© 2010, V. Lashkaryov Institute of Semiconductor Physics, National Academy of Sciences of Ukraine

9. M.A. Nicolet, Diffusion barriers in thin films // *Thin Solid Films* **52**(3), p. 415-443 (1978).
10. O.A. Ageev, A.E. Belyaev, N.S. Boltovets, R.V. Konakova, V.V. Milenin, V.A. Pilipenko, *Interstitial Phases in Technology for Semiconductor Devices and VLSI*, NTK "Institute of Single Crystals", Kharkov (2008) (in Russian).
11. V.N. Sheremet, The making features and electro-physical properties of ohmic contacts to gallium nitride (a review) // *Optoelektronika i Poluprovodnikovaya Tekhnika* **44**, p. 41-59 (2010) (in Russian).
12. Chung-Yu Ting, Charles Y. Chen, A study of the contacts of a diffused resistor // *Solid St. Electr*. **14**(6), p. 433-438 (1971).
13. V.N. Sheremet, Metrological aspects of measurement of ohmic contacts resistance // *Izvestiya Vuzov. Radioelektronika* **53**(3), p. 3-12 (2010) (in Russian).
14. R.H. Cox, H. Strack, Ohmic contacts for GaAs devices // *Solid St. Electr.* **10**(12), p. 1213-1218 (1967).
15. R.D. Brooks, H.G. Mattes, Spreading resistance between constant potential surfaces // *Bell Sys. Tech. J.* **50**(3), p. 775-784 (1971).
16. S.S. Cohen, Contact resistance and methods for its determination // *Thin Solid Films* **104**(3-4), p. 361-379 (1983).
17. E.B. Kaganovich, S.V. Svechnikov, The methods of measurement of contact resistance of semiconductor planar structures (a review) // *Optoelektronika i Poluprovodnikovaya Tekhnika* **21**, p. 1-11 (1991) (in Russian).
18. L.G. Russel, J.H. Michael, Y.R. Gary, The effect of lateral current spreading on the specific contact resistivity in D-Resistor Kelvin devices // *IEEE Trans. Electr. Dev.* **34**(3), p. 537-543 (1987).
19. N. Stavitski, M.J.H. van Dal, J.H. Klootwijk, R.A.M. Wolters, A.Y. Kovalgin, J. Schmitz, Cross-Bridge Kelvin Resistor (CBKR) structures for silicide-semiconductor junctions characterization, in *Proc. 9th Annual Workshop on Semiconductor Advances for Future Electronics and Sensors, 23-24 Nov 2006, Veldhoven, The Netherlands*, p. 436-438 (2006).
20. H.H. Berger, Contact resistance and contact resistivity // *J. Electrochem. Soc.* **119**(4), p. 507-514 (1972).
21. H.H. Berger, Models for contacts to planar devices // *Solid St. Electr.* **15**(2), p. 145-158 (1972).
22. H. Murrmann, D. Wiedmann, Current crowding on metal contacts to planar devices // *IEEE Trans. Electr. Dev.* **16**(12), p. 1022-1024 (1969).
23. H. Murrmann, D. Wiedmann, Messung des Übergangswiderstandes zwischen Metall und Diffusionsschicht in Si-Planarelementen // *Solid St. Electr.* **12**(11), p. 879-886 (1969).
24. G.K. Reeves, H.B. Harrison, Obtaining the specific contact resistance from transmission line model measurement // *IEEE Electron Device Lett.* **3**(5), p. 111-113 (1982).
25. A.N. Andreev, M.G. Rastegaeva, V.P. Rastegaev, S.A. Reshanov, To the problem of accounting for current spreading in a semiconductor when determining the transient resistance of ohmic contacts // *Fiz. Tekh. Poluprov.* **32**(7), p. 832-838 (1998) (in Russian).
26. G.K. Reeves, Specific contact resistance using a circular transmission line model // *Solid St. Electr.* **23**(5), p. 487-490 (1980).
27. D. Sawdai, Enhanced transmission line model structures for accurate resistance evaluation of small-size contacts and for more reliable fabrication // *IEEE Trans. Electron. Dev.* **46**(7), p. 1302-1311 (1999).
28. M. Lijadi, F. Pardo, N. Bardou, J. Pelouard, Floating contact transmission line modelling: An improved method for ohmic contact resistance measurement // *Solid St. Electr.* **49**(10) p. 1655-1661 (2005).
29. A.E. Belyaev, N.S. Boltovets, V.N. Ivanov, L.M. Kapitanchuk, V.P. Kladko, R.V. Konakova, Ya.Ya. Kudryk, A.V. Kuchuk, O.S. Lytvyn, V.V. Milenin, V.N. Sheremet, Yu.N. Sveshnikov, Development of high-stable contact systems to gallium nitride microwave diodes // *SQO* **10**(4), p. 1-8 (2007).
30. S. Noor Mohammad, Contact mechanisms and design principles for alloyed ohmic contacts to *n*-GaN // *J. Appl. Phys.* **95**(12), p. 7940-7953 (2004).
31. M. Pidun, P. Karduck, J. Mayer, K. Heime, B. Shineller, T. Walther, Auger depth profile analysis and EFTEM analysis of annealed Ti/Al-contacts on Si-doped GaN // *Appl. Surf. Sci*. **179**(1-4), p. 213-221 (2001).
32. S. Ruvimov, Z. Liliental-Weber, J. Washburn, D. Qiao, S.S. Lau, Paul K. Chu, Microstructure of Ti/Al ohmic contacts for *n*-AlGaN // *Appl. Phys. Lett.* **73**(18), p. 2582-2584 (1998).
33. W. Gotz, N.M. Johnson, C. Chen, H. Liu, C. Kuo, W. Imler, Activation energies of Si donors in GaN // *Appl. Phys. Lett.* **68**(22), p. 3144-3146 (1996).
34. A.E. Belyaev, N.S. Boltovets, V.N. Ivanov, V.P. Klad'ko, R.V. Konakova, Ya.Ya. Kudryk, A.V. Kuchuk, V.V. Milenin, Yu.N. Sveshnikov, V.N. Sheremet, On the tunnel mechanism of current flow in Au–TiB_x–*n*-GaN-*i*-Al_2O_3 Schottky barrier diodes // *SQO* **10**(3), p. 1-5 (2007).
35. V.V. Evstropov, Yu.V. Zhilyaev, M. Dzhumaeva, N. Nazarov, Tunnel-excess current in III–V nondegenerate barrier *p-n* and *m-s* structures on Si // *Fiz. Tekh. Poluprov.* **31**(2), p .152-158 (1997) (in Russian).
36. J.K. Shen, Y.K. Su, G.C. Chi, W.C. Chen, C.Y. Chen, C.N. Huang, J.M. Hong, Y.C. Yu, C.W. Wang, E.K. Lin, The effect of thermal annealing on thermal annealing on the Au/Ni contact of *p*-GaN // *J. Appl. Phys.* **83**(6), p. 3172-3175 (1998).
37. S.J. Pearton, F. Ren, A.P. Zhang, K.P. Lee, Fabrication and performance of GaN electronic devices // *Mat. Sci. Eng. R* **30**(3-6), p. 55-212 (2000).

© 2010, V. Lashkaryov Institute of Semiconductor Physics, National Academy of Sciences of Ukraine